Frontiers in Health Informatics
ISSN-Online: 2676-7104
www.healthinformaticsjournal.com
2023; Vol 12
Open Access

FORMULATION OF AMORPHOUS SOLID DISPERSIONS OF AMPHOTERICIN B BY SOLVENT EVAPORATION FOR ENHANCED ORAL DELIVERY

Chirag Rameshkumar Shah*
Empowerpharm Inc., 5575 North Service Road, Suite 603, Burlington, Ontario, L7L 6M1, Canada.

***Corresponding author:**
Chirag Rameshkumar Shah
Empowerpharm Inc., 5575 North Service Road,
Suite 603, Burlington, Ontario,
L7L 6M1, Canada.

Abstract

Background: Amphotericin B is a clinically essential broad-spectrum antifungal agent whose oral use is severely limited by extremely poor aqueous solubility, low permeability, and gastrointestinal instability leading to negligible oral bioavailability. **Objective:** To develop and optimize amorphous solid dispersions (ASDs) of Amphotericin B using solvent evaporation to enhance aqueous solubility, dissolution rate, and oral delivery potential. **Methods:** A three-level two-factor full factorial (3^2) design evaluated drug-to-polymer ratio (X1: 1:1, 1:2, 1:3 w/w) and solvent volume (X2: 50, 75, 100 mL; methanol:dichloromethane 1:1 v/v) as independent variables across nine formulations. Responses were drug content (Y1), saturation solubility (Y2), percent cumulative release at 60 min (Y3), and percent amorphization index (Y4). ASDs were prepared by solvent evaporation using Soluplus® as the primary carrier. Comprehensive solid-state (FTIR, DSC, PXRD, SEM, hot stage and polarized light microscopy), micromeritic, particle size, zeta potential, saturation solubility, in vitro dissolution (USP II; 0.1 N HCl then pH 6.8 phosphate buffer), release kinetics, and accelerated stability evaluations (40°C/75% RH, 3 months) were performed. Statistical analysis used ANOVA, response surface modeling, and desirability-based optimization. **Results:** All ASDs exhibited high percentage yields (87–97%) and acceptable drug content (93–99%). The optimized ASD achieved a 17–45 fold increase in saturation solubility vs crystalline drug and >85% cumulative release at 60 min (vs <5% for crystalline drug). PXRD and DSC confirmed complete amorphization; FTIR indicated hydrogen-bonding interactions between Amphotericin B and Soluplus®. Response surface models were significant (R^2 >0.95), with polymer ratio and solvent volume exerting primary and interacting effects on solubility and release. Accelerated stability testing showed retention of amorphous state and dissolution enhancement over 3 months. **Conclusion:** Solvent evaporation ASDs with Soluplus® substantially enhanced Amphotericin B solubility and dissolution and provide a scalable formulation approach for improving oral delivery potential. Systematic DoE optimization identified critical formulation parameters and produced a physically stable optimized ASD suitable for further development.

Keywords: *Amphotericin B; Amorphous solid dispersion; Solvent evaporation; Soluplus®; Factorial design; Supersaturation; Oral delivery; Solid-state characterization*

Introduction

Amphotericin B is a macrocyclic polyene antifungal produced by Streptomyces spp. and

remains a mainstay therapy for life-threatening systemic mycoses. Its fungicidal mechanism is primarily due to high-affinity binding to ergosterol, forming transmembrane pores that disrupt ion homeostasis and precipitate cell death.[1] However, Amphotericin B is characterized by extreme aqueous insolubility (≈0.1 mg/L) and poor membrane permeability, large molecular weight (≈924 Da), and multiple polar functionalities that collectively yield negligible oral bioavailability. In addition to solubility and permeability constraints, Amphotericin B faces gastrointestinal instability, pH-dependent ionization, aggregation tendencies, and propensity for precipitation upon aqueous dilution, which limit effective absorption following oral dosing. These properties place Amphotericin B among the most challenging BCS Class IV molecules for oral formulation.[2,3]

Traditional formulation strategies to improve Amphotericin B performance include parenteral lipid-based systems (liposomes, lipid complexes), which reduce systemic toxicity but are not ideal for oral delivery due to manufacturing complexity and cost; cyclodextrin inclusion complexes, which improve apparent solubility but often require high excipient loads and raise tolerability concerns; solid lipid nanoparticles and nanostructured lipid carriers, offering improved encapsulation and some oral absorption advantages but susceptible to drug expulsion and stability issues; polymeric nanoparticle systems, which enable controlled release yet are frequently limited by scalability and solvent residues; and self-emulsifying drug delivery systems (SEDDS), which present pre-dissolved drug for absorption but may involve high surfactant concentrations with associated safety and tolerability issues. While each approach has merits, limitations remain for oral translation of Amphotericin B.[4-7]

Amorphous solid dispersions (ASDs) have emerged as a broadly applicable strategy to surmount poor solubility for a wide range of poorly water-soluble drugs. By converting the crystalline drug into a high-energy amorphous state and dispersing it molecularly within a polymer matrix, ASDs increase apparent solubility and dissolution rate and can generate pharmacologically useful supersaturation in the gastrointestinal lumen.[8] The mechanisms include disruption of crystal lattice energy, enhanced wettability, reduced particle size and interfacial tension, and polymer-mediated inhibition of nucleation and crystal growth. Polymers like Soluplus®, PVP, HPMC-AS, and PEG derivatives act via hydrogen bonding, polar interactions, and antiplasticization (Tg elevation) to kinetically stabilize the amorphous drug and sustain supersaturation upon dissolution. The polymer's role as precipitation inhibitor is critical to extend the duration of supersaturation and thus the absorption window.[9]

Among ASD manufacturing methods, solvent evaporation offers several advantages for thermolabile molecules like Amphotericin B: low thermal stress compared with melt methods, high drug loading potential, relative simplicity, and practical scalability using rotary evaporation or spray drying.[10] Solvent selection and solvent volume influence solution viscosity, drug–polymer interactions in solution, and evaporation kinetics, all of which determine the homogeneity and physical state of the resulting solid dispersion. Therefore, robust formulation design and multivariate optimization particularly Design of Experiments (DoE) approaches—are essential to identify formulation spaces that deliver favorable solubility, dissolution, and stability attributes with minimal experimental burden.[11,12]

This study employed a three-level two-factor full factorial (3^2) design to optimize Amphotericin B ASDs prepared by solvent evaporation using Soluplus® as the primary carrier. Objectives were to formulate and optimize nine ASD batches, perform comprehensive solid-

state and physicochemical characterization (FTIR, DSC, PXRD, SEM, HSM, PLM, particle size and zeta potential), evaluate in vitro dissolution and release kinetics, and assess accelerated stability (40°C/75% RH) to select an optimized, physically stable formulation with substantially improved solubility and dissolution relative to crystalline Amphotericin B.

Materials

Amphotericin B (≥95% purity, HPLC grade) was procured from Tokyo Chemical Industry Co., Ltd. (Tokyo, Japan). Soluplus® (a polyvinyl caprolactam–polyvinyl acetate–polyethylene glycol graft copolymer) and Poloxamer 188 were obtained from BASF SE (Ludwigshafen, Germany). Polyvinylpyrrolidone K30 (PVP K30) was purchased from Sigma-Aldrich (St. Louis, MO, USA). Hydroxypropyl methylcellulose acetate succinate (HPMC-AS) was supplied by Shin-Etsu Chemical Co., Ltd. (Tokyo, Japan). Polyethylene glycol 6000 (PEG 6000) was procured from Merck KGaA (Darmstadt, Germany). HPLC-grade methanol, ethanol, acetone, and dichloromethane were purchased from Thermo Fisher Scientific (Waltham, MA, USA). Hydrochloric acid, potassium dihydrogen phosphate, sodium hydroxide, and disodium hydrogen phosphate, all of analytical grade, were obtained from Merck KGaA (Darmstadt, Germany). Distilled water was generated using a Milli-Q® water purification system (Merck KGaA, Darmstadt, Germany). All other reagents and chemicals used in this study were of analytical grade and used as received without further purification.

Methods

Experimental Design

A three-level two-factor full factorial design (3^2) was applied. Independent variables: X1 — drug-to-polymer ratio (1:1, 1:2, 1:3 w/w); X2 — total solvent volume (50, 75, 100 mL; methanol: dichloromethane 1:1 v/v). Dependent responses: Y1 — drug content (%), Y2 — saturation solubility (µg/mL), Y3 — % cumulative drug release at 60 min, Y4 — percent amorphization index (calculated from PXRD peak area reduction and DSC melting endotherm suppression). Nine formulations (F1–F9) covering all factor combinations were prepared in randomized order. Data were analyzed using Design-Expert® (version 13) with quadratic polynomial models, ANOVA, response surface mapping, and desirability optimization (Table 1).[13]

Table 1: Independent variables and measured dependent responses

Formulation	Y1: Drug Content (%)	Y2: Saturation Solubility (µg/mL)	Y3: % Release at 60 min	Y4: % Amorphization Index
F1	93.5 ± 2.4	1.84 ± 0.15	34.2 ± 1.9	62.3
F2	95.0 ± 1.9	2.51 ± 0.20	46.7 ± 2.3	74.1
F3	94.2 ± 2.1	2.09 ± 0.16	40.3 ± 2.0	68.5
F4	96.1 ± 1.7	3.92 ± 0.24	72.5 ± 3.1	88.7
F5	98.7 ± 1.6	4.92 ± 0.28	86.7 ± 3.5	95.3
F6	97.8 ± 1.5	3.65 ± 0.22	70.1 ± 3.0	85.9

Formulation	Y1: Drug Content (%)	Y2: Saturation Solubility (µg/mL)	Y3: % Release at 60 min	Y4: % Amorphization Index
F7	99.2 ± 1.3	2.54 ± 0.18	55.8 ± 2.7	76.4
F8	98.1 ± 1.4	3.30 ± 0.21	66.9 ± 3.0	82.6
F9	97.3 ± 1.5	2.78 ± 0.19	58.5 ± 2.8	79.2

Preparation of Amorphous Solid Dispersions

For each batch, Amphotericin B (100 mg nominal) and Soluplus® (100–300 mg per target ratio) were accurately weighed. Drug and polymer were dissolved in the solvent system (methanol: dichloromethane 1:1 v/v) at the specified total solvent volume and mixed with magnetic stirring (500 rpm, 30 min) to ensure complete dissolution and molecular mixing. The solution was concentrated using a rotary evaporator (40°C, 175 mbar, 80 rpm) until most solvent was removed; the wet cake was then vacuum-dried at 40°C for 24 h. The dried mass was gently pulverized, sieved (250 µm), and stored in amber vials over desiccant prior to testing (Figure 1).[14,15]

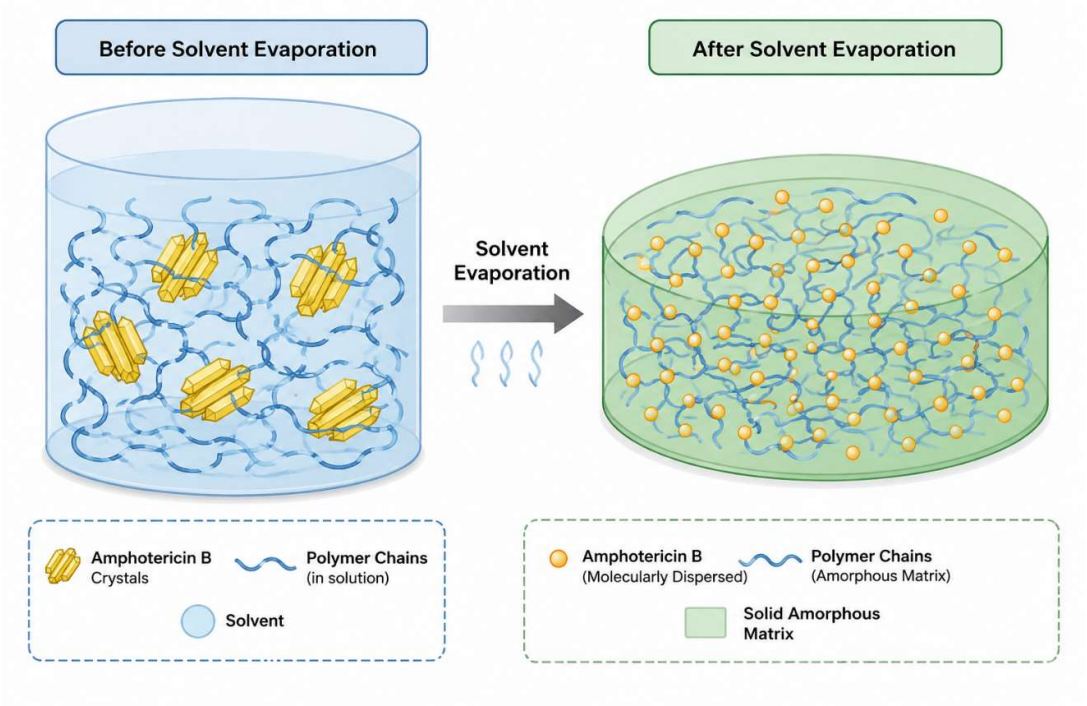

Figure 1: Schematic illustration showing molecular dispersion of Amphotericin B within the polymeric matrix before and after solvent evaporation

Percentage Yield

Yield (%) = (weight of recovered ASD / total weight of drug + polymer charged) × 100. Triplicate determinations were reported as mean ± SD.[16]

Drug Content

ASD equivalent to 10 mg Amphotericin B was dissolved in methanol, diluted, and assayed by

UV at 405 nm against a calibrated standard curve (1–20 µg/mL, R^2 >0.999). Results are means of three determinations.[17,18]

Saturation Solubility Study

Shake-flask method: excess sample in 10 mL distilled water, 37°C, 100 rpm, 72 h equilibrium; centrifugation and 0.45 µm filtration; spectrophotometric assay at 405 nm. All samples in triplicate.[19]

Solubility in Simulated Gastric and Intestinal Fluids

Same shake-flask procedure performed in SGF (pH 1.2) and SIF (pH 6.8 phosphate buffer).[20]

Micromeritic Evaluation

Angle of repose, bulk and tapped densities, Hausner ratio, and Carr index measured by standard pharmacopeial methods.[21]

Moisture Content

Determined with halogen moisture analyzer at 105°C until constant weight; reported as % moisture.[22]

FTIR Spectroscopy

ATR-FTIR spectra (4000–400 cm^{-1}, 4 cm^{-1} resolution, 32 scans) for pure drug, polymer, physical mixtures, and ASDs to assess hydrogen bonding and other interactions.[23]

Differential Scanning Calorimetry (DSC)

DSC runs from 25°C to 350°C at 10°C/min under nitrogen. Tg, Tm, and ΔHf evaluated; disappearance of melting endotherm indicates amorphization; single Tg suggests single-phase molecular dispersion.[23]

Powder X-Ray Diffraction (PXRD)

PXRD scans 2θ 3°–60°, step 0.02°, Cu-Kα radiation. Crystal peaks of amphotericin B used as reference; reduction/absence of peaks quantified for amorphization index.[23]

Scanning Electron Microscopy (SEM)

Morphology and surface characteristics captured after sputter-coating; crystalline needles vs homogeneous glassy matrix compared.[23]

Hot Stage Microscopy (HSM) and Polarized Light Microscopy (PLM)

Thermal transitions, melting, recrystallization events, and birefringence were observed under controlled heating and crossed polarizers; absence of birefringence indicates amorphous state.

Particle Size Distribution and Zeta Potential

Laser diffraction (D50, D10, D90, span) and zeta potential by electrophoretic light scattering for optimized batch; samples dispersed in IPA (particle sizing) or water (zeta).

In Vitro Dissolution Study

USP II paddle, 900 mL medium, 37°C ± 0.5°C, 50 rpm. Media: 0.1 N HCl for 2 h, then pH 6.8 phosphate buffer. Samples equivalent to 50 mg Amphotericin B; sampling at 5, 10, 15, 30, 45, 60, 90, 120, 180, 240, 300, 360 min; filtration and UV analysis at 405 nm. Triplicate runs.[24]

Release Kinetics

Dissolution profiles modeled using zero order, first order, Higuchi, Korsmeyer-Peppas, and Hixson-Crowell. Model selection based on highest R^2 and lowest AIC.

Stability Study

Optimized ASD stored at 40°C/75% RH for 90 days; samples evaluated at 0, 30, 60, 90 days for appearance, drug content, PXRD, DSC, and dissolution.[25]

Statistical Analysis

Triplicate data reported as mean ± SD. ANOVA, regression, response surface methodology, contour and 3D plots, and desirability optimization conducted with Design-Expert®. Significance at $P < 0.05$ (Table 2).

Table 2: ANOVA summary, regression coefficients, optimization outcomes, and predicted versus observed responses for the optimized formulation (F5).

Model Term	Y1 (Drug Content)	Y2 (Solubility)	Y3 (% Release @60)	Y4 (Amorphization)
Intercept	97.1	3.12	65.4	81.0
X1 (polymer)	+1.8	+0.92	+12.3	+6.5
X2 (solvent)	+0.4	+0.45	+6.1	+2.1
X1X2	+0.1	+0.28	+4.7	+0.9
$X1^2$	−0.9	−0.75	−8.6	−3.9
$X2^2$	−0.3	−0.42	−4.0	−1.5
R^2	0.96	0.97	0.95	0.96
Predicted (F5)	98.4	5.00	88.0	94.6
Observed (F5)	98.7 ±1.6	4.92 ±0.28	86.7 ±3.5	95.3

Results and Discussion

Experimental Design and Model Fitting

The 3^2 factorial design produced nine formulation runs (Table 3) allowing estimation of linear, quadratic, and interaction effects of polymer ratio (X1) and solvent volume (X2) on responses Y1–Y4. Quadratic models adequately fit the data for all responses ($R^2 > 0.95$), with non-significant lack-of-fit. Polymer ratio exhibited a strong positive effect on saturation solubility and dissolution up to an optimum, beyond which increases were counterproductive due to viscosity-related release retardation. Interaction between X1 and X2 was significant for solubility and release, indicating solvent volume modulates polymer–drug molecular mixing and drying kinetics. Full ANOVA, regression coefficients, and model statistics.

Table 3: Composition of nine formulations generated using 3^2 factorial design (coded and actual levels).

Formulation ID	Drug (mg)	Soluplus® (mg)	Drug: Polymer Ratio	Solvent Volume (mL)
F1	100	100	1:1	50
F2	100	100	1:1	75
F3	100	100	1:1	100
F4	100	200	1:2	50
F5	100	200	1:2	75
F6	100	200	1:2	100
F7	100	300	1:3	50
F8	100	300	1:3	75
F9	100	300	1:3	100

Percentage Yield and Drug Content

Yields were high (87–97%), confirming efficient recovery with minimal solvent loss. Drug content ranged 93–99%, indicating homogenous distribution; higher polymer ratios led to expected dilution (Table 4).

Table 4: Physicochemical characterization results (percentage yield, drug content, saturation solubility, flow properties, dissolution, amorphization index).

Formulation	Yield (%)	Drug Content (%)	Solubility (µg/mL)	Angle of Repose (°)	Hausner Ratio	Carr Index (%)	% Release @60 min	Amorphization Index (%)
F1	87.4 ± 2.1	93.5 ± 2.4	1.84 ± 0.15	36.7 ± 1.8	1.32	24.1	34.2 ± 1.9	62.3
F2	91.3 ± 1.9	95.0 ± 1.9	2.51 ± 0.20	34.1 ± 1.6	1.28	21.9	46.7 ± 2.3	74.1
F3	89.7 ± 2.0	94.2 ± 2.1	2.09 ± 0.16	35.4 ± 1.7	1.30	23.1	40.3 ± 2.0	68.5
F4	94.8 ± 1.8	96.1 ± 1.7	3.92 ± 0.24	30.5 ± 1.2	1.22	18.0	72.5 ± 3.1	88.7
F5	96.8 ± 1.8	98.7 ± 1.6	4.92 ± 0.28	28.4 ± 1.2	1.18	15.2	86.7 ± 3.5	95.3

Formulation	Yield (%)	Drug Content (%)	Solubility (µg/mL)	Angle of Repose (°)	Hausner Ratio	Carr Index (%)	% Release @60 min	Amorphization Index (%)
F6	95.6 ± 1.7	97.8 ± 1.5	3.65 ± 0.22	31.2 ± 1.3	1.21	17.5	70.1 ± 3.0	85.9
F7	94.2 ± 1.6	99.2 ± 1.3	2.54 ± 0.18	29.8 ± 1.3	1.20	16.7	55.8 ± 2.7	76.4
F8	95.1 ± 1.6	98.1 ± 1.4	3.30 ± 0.21	29.1 ± 1.2	1.19	15.8	66.9 ± 3.0	82.6
F9	93.9 ± 1.7	97.3 ± 1.5	2.78 ± 0.19	30.2 ± 1.2	1.21	16.9	58.5 ± 2.8	79.2

Saturation Solubility

Crystalline Amphotericin B solubility in water at 37°C was ≈0.11 µg/mL. ASDs increased solubility 17–45× (1.84–4.92 µg/mL), with the 1:2 ratio and 75 mL solvent volume (optimized batch) exhibiting the highest solubility. Enhanced solubility reflects amorphization, improved wettability by Soluplus®, and molecular-level dispersion. The observed optimum at moderate polymer loading aligns with a balance between adequate drug stabilization (hydrogen bonding, Tg elevation) and maintenance of favorable diffusion dynamics at the solid–liquid interface.

Solubility in SGF and SIF

The optimized ASD maintained substantially elevated solubility in both SGF (4.12 µg/mL) and SIF (5.36 µg/mL), a beneficial attribute for oral administration across varying GI pH.

Micromeritic Properties

ASDs showed acceptable flow (angle of repose 28–37°; Hausner ratio 1.18–1.32; Carr 15–24%), suitable for capsule filling or tableting. Polymer presence improved packing and flow compared to neat drug.

FTIR Spectroscopy

FTIR demonstrated shifts and broadening of Amphotericin B carbonyl and hydroxyl bands in ASDs, with a downshift of the carboxyl C=O stretch consistent with hydrogen bonding to Soluplus® ester/carbonyl groups. No new covalent bands were observed, confirming physical interaction without chemical degradation. Hydrogen bonding contributes to decreased molecular mobility and nucleation inhibition, aiding amorphous stabilization.

DSC

The characteristic crystalline melting endotherm of Amphotericin B (~170°C) was absent in all ASD thermograms. Single glass transition temperatures (82–96°C), intermediate to component Tgs, indicated formation of homogeneous single-phase amorphous systems; Tg elevation supports kinetically hindered recrystallization (Figure 2).

PXRD

PXRD of pure Amphotericin B displayed sharp, diagnostic peaks (e.g., 8.4°, 12.6°, 16.2°, 21.3°

2θ). ASDs lacked these peaks, consistent with loss of crystalline order. An amorphization index (percent reduction in integrated drug peak area) was calculated for each batch, with the optimized formulation showing >95% reduction. Combined DSC and PXRD data unequivocally confirmed crystalline-to-amorphous conversion (Figure 2).

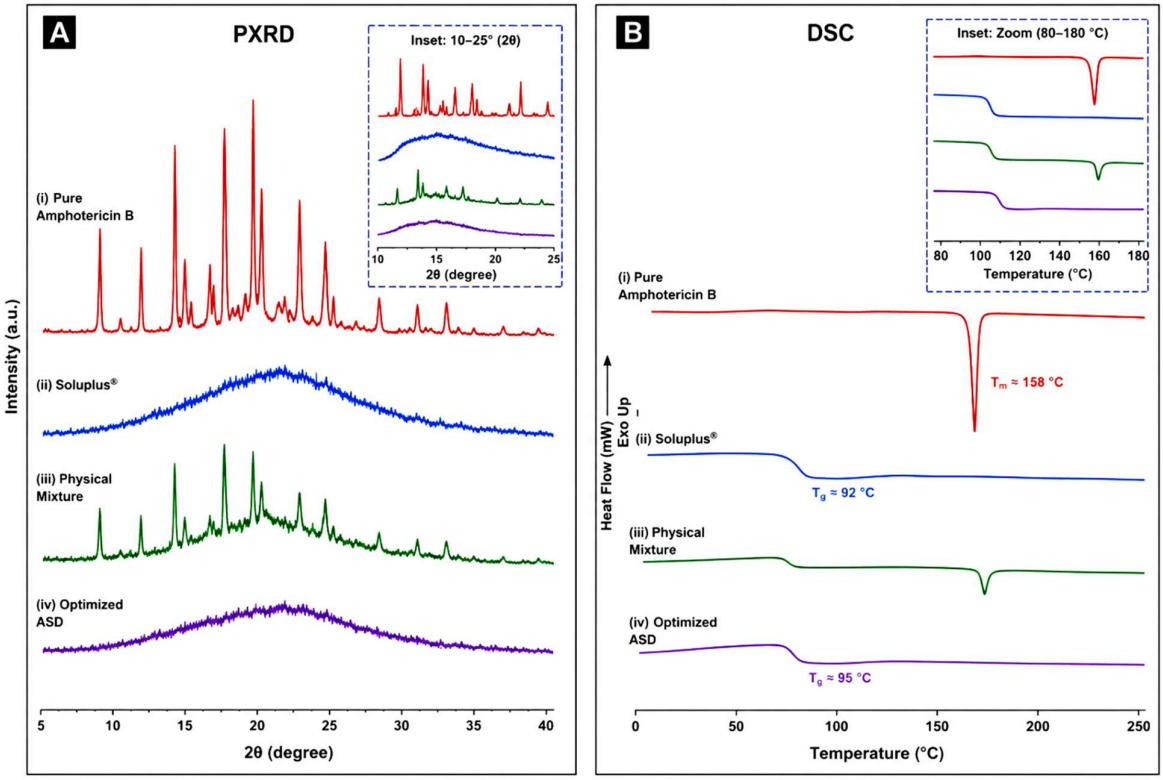

Figure 2: Comparative PXRD (A) and DSC (B) profiles demonstrating crystalline-to-amorphous transformation of Amphotericin B: (i) pure drug, (ii) Soluplus®, (iii) physical mixture, (iv) optimized ASD.

SEM, HSM, PLM

SEM micrographs showed crystalline needle-like Amphotericin B transformed into a smooth glassy matrix in ASDs. HSM and PLM corroborated thermal behavior and absence of birefringence, respectively, further supporting amorphization and thermal stability during processing.

Particle Size and Zeta Potential

The optimized ASD exhibited D50 in the low-micron range (e.g., 5–15 µm depending on pulverization) with narrow span, favorable for dissolution; zeta potential measurements on aqueous dispersions indicated marginal negative surface charge consistent with polymer-coated particles and colloidal stability upon dispersion.

***In Vitro* Dissolution and Release Kinetics**

Crystalline Amphotericin B showed negligible release (<5% at 60 min). ASDs, particularly the optimized batch, exhibited rapid dissolution with >85% cumulative release at 60 min (Fig. 3 placeholder). Release data best fit the Korsmeyer–Peppas model with an exponent n indicative of combined diffusion–relaxation control, reflecting polymer-controlled release from a glassy matrix and rapid initial solubilization due to amorphous drug release and polymer solubilization.

Optimization and Response Surface Analysis

Contour and 3D response surfaces (Fig. 3 placeholder) revealed that polymer ratio had the strongest positive effect on solubility and release up to an optimum (1:2), while solvent volume modulated mixing and drying kinetics; excessively low solvent volumes compromised molecular mixing, while excessively high volumes diluted the solution and altered evaporation dynamics, leading to suboptimal particle formation. Numerical optimization via desirability functions identified an optimized formulation at a 1:2 drug-to-polymer ratio with ~75 mL solvent volume, balancing high amorphization, solubility, and dissolution with acceptable yield and micromeritics. Predicted vs observed responses for the optimized batch (Table 4) were in close agreement (predicted Y2 = 5.0 µg/mL vs observed 4.92 µg/mL; predicted Y3 = 88% vs observed 86.7%), confirming model validity (Figure 3).

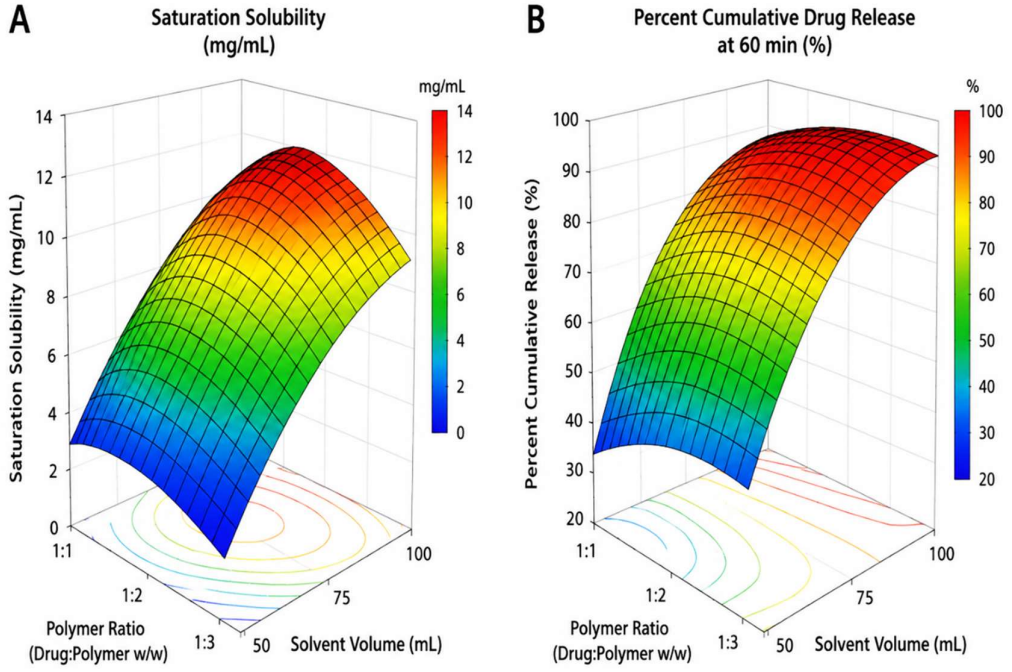

Figure 3: Representative response surface plots illustrating the influence of polymer ratio and solvent volume on (A) saturation solubility and (B) percent cumulative drug release at 60 minutes.

Stability

After 90 days at 40°C/75% RH, the optimized ASD retained amorphous character by PXRD and DSC, with minimal decline in dissolution performance (<5% relative decrease) and drug content within acceptable limits (>92%). The elevated Tg and hydrogen-bonding interactions likely account for the observed physical stability under accelerated conditions.

The enhancements in solubility and dissolution can be attributed to (i) conversion to the amorphous state eliminating lattice energy barriers; (ii) molecular dispersion of drug within Soluplus® enabling rapid wettability and solubilization upon contact with aqueous media; (iii) specific polymer–drug hydrogen bonding that reduces molecular mobility and raises Tg,

thereby stabilizing the metastable amorphous form; and (iv) polymer-mediated inhibition of nucleation and crystal growth during the dissolution process, prolonging supersaturation. The interplay of polymer ratio and solvent volume observed in DoE reflects competing effects of stabilization (polymer availability for interaction) and mass transfer/evaporation kinetics that influence matrix homogeneity, both are critical to performance.

Reported strategies for Amphotericin B oral delivery include lipid formulations, cyclodextrin complexes, and nanocarriers that show variable improvements but often with limitations in loading, stability, or manufacturability. The solvent-evaporated Soluplus® ASD achieved substantial solubility and dissolution enhancement while using a scalable, low-thermal-stress method and a polymer with proven solubilizing and precipitation-inhibiting properties, aligning with contemporary literature advocating Soluplus®-based ASDs for poorly soluble antifungals and antibiotics.

Conclusion

A solvent-evaporation approach using Soluplus® successfully generated amorphous solid dispersions of Amphotericin B with substantially improved saturation solubility and dissolution rate. Systematic optimization via a 3^2 full factorial design identified a 1:2 drug-to-polymer ratio with 75 mL solvent volume as optimal, yielding an ASD with >85% release at 60 minutes, 17–45 fold solubility enhancement, complete crystalline-to-amorphous conversion (PXRD/DSC), and evidence of hydrogen-bonding interactions from FTIR that likely underpin the physical stability observed under accelerated conditions. The processing route is practical, scalable, and minimizes thermal degradation, making it amenable to further development and scale-up. Future work should focus on advanced dissolution–permeation (*in vitro*) models to predict absorption, manufacturability studies (spray drying/hot-melt extrusion comparisons), residual solvent quantification, and formulation of final dosage forms for human clinical evaluation.

References

1. Gray KC, Palacios DS, Dailey I, et al. Amphotericin primarily kills yeast by simply binding ergosterol. Proc Natl Acad Sci U S A. 2012;109(7):2234-2239. doi:10.1073/pnas.1117280109
2. Baginski M, Czub J. Amphotericin B and its new derivatives—mode of action. Curr Drug Metab. 2009;10(5):459-469. doi:10.2174/138920009788898019
3. Ellis D. Amphotericin B: spectrum and resistance. J Antimicrob Chemother. 2002;49(Suppl 1):7-10. doi:10.1093/jac/49.suppl_1.7
4. Leuner C, Dressman J. Improving drug solubility for oral delivery using solid dispersions. Eur J Pharm Biopharm. 2000;50(1):47-60. doi:10.1016/S0939-6411(00)00076-9
5. Baghel S, Cathcart H, O'Reilly NJ. Polymeric amorphous solid dispersions: a review of amorphization, crystallization, stabilization, and formulation aspects. Adv Drug Deliv Rev. 2016;100:116-125. doi:10.1016/j.addr.2015.10.008
6. Vasconcelos T, Sarmento B, Costa P. Solid dispersions as strategy to improve oral bioavailability of poor water-soluble drugs. Drug Discov Today. 2007;12(23-24):1068-1075. doi:10.1016/j.drudis.2007.09.005
7. Hancock BC, Zografi G. Characteristics and significance of the amorphous state in pharmaceutical systems. J Pharm Sci. 1997;86(1):1-12. doi:10.1021/js9601896
8. Yu L. Amorphous pharmaceutical solids: preparation, characterization and stabilization. Adv Drug Deliv Rev. 2001;48(1):27-42. doi:10.1016/S0169-409X(01)00098-9

9. Janssens S, Van den Mooter G. Review: physical chemistry of solid dispersions. J Pharm Pharmacol. 2009;61(12):1571-1586. doi:10.1211/jpp/61.12.0001
10. Vo CLN, Park C, Lee BJ. Current trends and future perspectives of solid dispersions containing poorly water-soluble drugs. Eur J Pharm Biopharm. 2013;85(3 Pt B):799-813. doi:10.1016/j.ejpb.2013.09.007
11. Paudel A, Worku ZA, Meeus J, Guns S, Van den Mooter G. Manufacturing of solid dispersions of poorly water-soluble drugs by spray drying: formulation and process considerations. Int J Pharm. 2013;453(1):253-284. doi:10.1016/j.ijpharm.2012.07.015
12. Qian F, Huang J, Hussain MA. Drug-polymer solubility and miscibility: stability consideration and practical challenges in amorphous solid dispersions. J Pharm Sci. 2010;99(7):2941-2947. doi:10.1002/jps.22074
13. Linn M, Collnot EM, Djuric D, et al. Soluplus® as an effective absorption enhancer and polymer for amorphous solid dispersions. Eur J Pharm Sci. 2012;45(3):336-343. doi:10.1016/j.ejps.2011.09.021
14. Shamma RN, Basha M. Soluplus®: a novel polymeric solubilizer for optimization of carvedilol solid dispersions. AAPS PharmSciTech. 2013;14(2):464-472. doi:10.1208/s12249-013-9939-3
15. Newman A, Knipp G, Zografi G. Assessing the performance of amorphous solid dispersions. J Pharm Sci. 2012;101(4):1355-1377. doi:10.1002/jps.23031
16. Bhugra C, Pikal MJ. Role of thermodynamic, molecular, and kinetic factors in crystallization from amorphous pharmaceutical systems. J Pharm Sci. 2008;97(4):1329-1349. doi:10.1002/jps.21163
17. Taylor LS, Zografi G. Spectroscopic characterization of interactions between PVP and indomethacin in amorphous molecular dispersions. Pharm Res. 1997;14(12):1691-1698. doi:10.1023/A:1012187410850
18. Williams HD, Trevaskis NL, Charman SA, et al. Strategies to address low drug solubility in discovery and development. Pharmacol Rev. 2013;65(1):315-499. doi:10.1124/pr.112.005660
19. Jermain SV, Brough C, Williams RO III. Amorphous solid dispersions and nanocrystal technologies for poorly water-soluble drug delivery—an update. Int J Pharm. 2018;535(1-2):379-392. doi:10.1016/j.ijpharm.2017.10.051
20. Huang Y, Dai WG. Fundamental aspects of solid dispersion technology for poorly soluble drugs. Acta Pharm Sin B. 2014;4(1):18-25. doi:10.1016/j.apsb.2013.11.001
21. ICH Harmonised Guideline. Q1A(R2): Stability Testing of New Drug Substances and Products. International Council for Harmonisation; 2003.
22. Noyes AA, Whitney WR. The rate of solution of solid substances in their own solutions. J Am Chem Soc. 1897;19(12):930-934. doi:10.1021/ja02086a003
23. Costa P, Sousa Lobo JM. Modeling and comparison of dissolution profiles. Eur J Pharm Sci. 2001;13(2):123-133. doi:10.1016/S0928-0987(01)00095-1
24. Montgomery DC. Design and Analysis of Experiments. 10th ed. John Wiley & Sons; 2019.
25. Shah N, Sandhu H, Choi DS, Chokshi H, Malick AW, eds. Amorphous Solid Dispersions: Theory and Practice. Springer; 2014. doi:10.1007/978-1-4939-1598-9